

**Supporting Information for**

**Dielectric Relaxation and Solvation Dynamics in a Prototypical Ionic Liquid +  
Dipolar Protic Liquid Mixture:  
1-Butyl-3-Methylimidazolium Tetrafluoroborate + Water**

**Xin-Xing Zhang,<sup>1,2</sup> Min Liang,<sup>3</sup> Johannes Hunger,<sup>4</sup> Richard Buchner,<sup>4</sup> and Mark  
Maroncelli<sup>3\*</sup>**

**<sup>1</sup>Department of Physics, Nankai University, Tianjin, China**

**<sup>2</sup>Department of Chemistry, Humboldt Universität zu Berlin, Germany**

**<sup>3</sup>Department of Chemistry, The Pennsylvania State University, University Park, PA, USA**

**<sup>4</sup>Institut für Physikalische und Theoretische Chemie, Universität Regensburg, 93040  
Regensburg, Germany**

**A) Dielectric Parameters:** Figure S1 shows the dependence of three parameters characterizing global aspects of the permittivity spectra,  $\epsilon_\infty$ ,  $\epsilon = \epsilon_\infty + \sum S_j$ , and  $\langle \tau_{diel} \rangle = \sum_j S_j \tau_j / \sum_j S_j$ , on ionic liquid mole fraction ( $x_{IL}$ ) and volume fraction ( $\Phi_{IL}$ ). The non-monotonic behavior of  $\epsilon_\infty$  and in  $\langle \tau_{diel} \rangle$  at high  $\Phi_{IL}$  probably only reflect uncertainties in the data and fits.

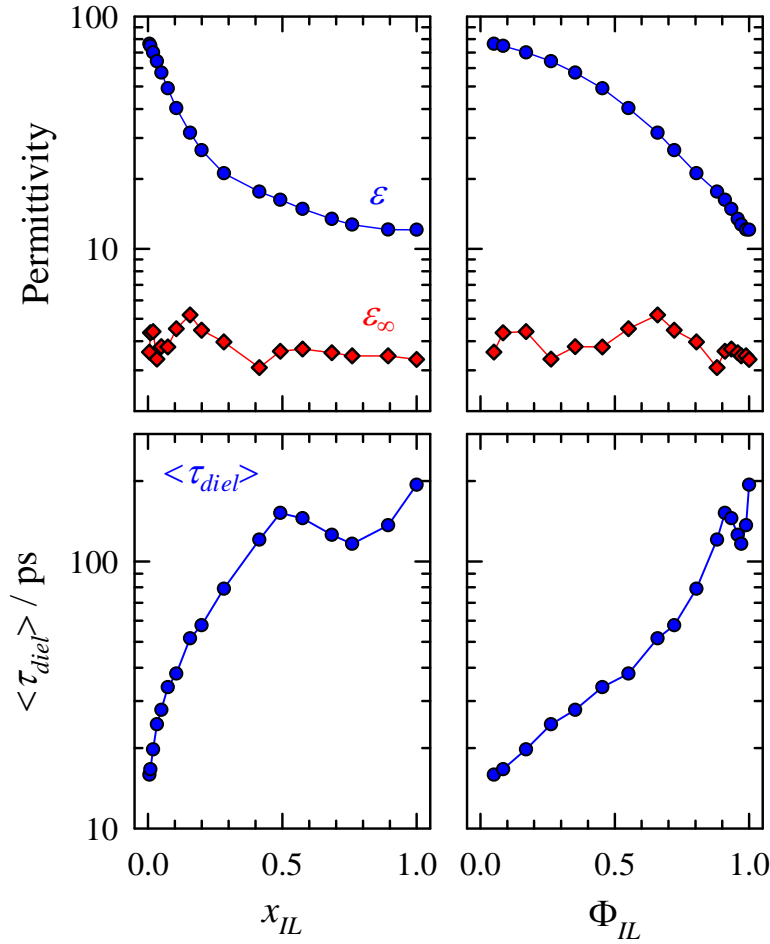


**Fig. S1:** Composition dependence of the three parameters characterizing the global permittivity spectra:  $\epsilon_\infty$ ,  $\epsilon$ , and  $\langle \tau_{diel} \rangle$ .

**B) Viscosities at 20.5 °C:** Because the spectroscopic experiments were conducted at  $20.5 \pm 1$  °C rather than at 25 °C where dielectric and other data are available, we measured solution viscosities at this temperature to determine the expected effect on dynamics. Viscosities were measured using several Cannon-Fenske glass viscometers immersed in a thermostated bath ( $\pm 0.1$  °C). Kinematic viscosities were transformed into shear viscosities using the density data of

Taib *et al.*<sup>1</sup> Results are listed in Table S1 and compared to the fitted data at 25 °C from Fig. 2 in Fig. S2.

**Table S1: Viscosities at 20.5 °C**

$x_{IL}$	$\eta$ /mPa s
0	1.00
0.10	3.1
0.30	8.2
0.50	16.9
0.70	36.6
0.90	78.5
1.00	130

Uncertainties <5%.

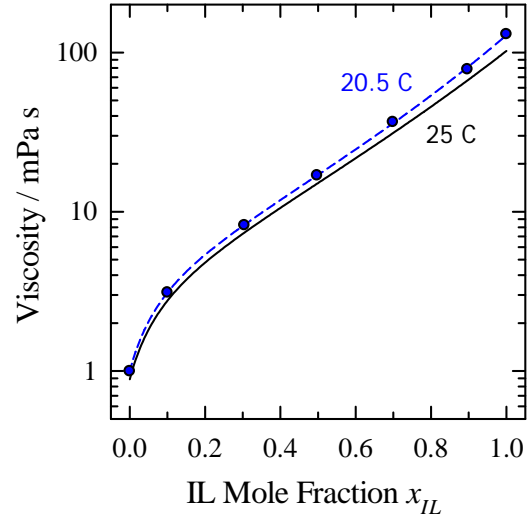


**Fig. S2:** Measured (points) viscosities at 20.5 °C compared to the fit to literature data (solid black curve) at 25 °C. Dashed blue line is similar fit of 20.5 °C data.

The viscosities measured here at 20.5 °C show a nearly identical composition dependence to those measured at 25 °C but are higher by an average of 15% (from 13% in pure water to 25% in pure [Im<sub>41</sub>][BF<sub>4</sub>]). Similar differences are expected for solvation dynamical quantities measured at 20.5 versus 25 °C. Such differences are of little consequence for the comparisons being made between solvation and dielectric data.

**C) Spectral Response Function Fits:** The  $S_v(t)$  data were fit to two different functions, a 4-parameter Gaussian + stretched exponential function

$$S_v(t) = f_G \exp(-\frac{1}{2} \omega_G^2 t^2) + (1 - f_G) \exp\{-(t/\tau)^\beta\} \quad (\text{S1})$$

and a 5-parameter triple exponential function

$$S_v(t) = \sum_{i=1}^3 f_i \exp(-t/\tau_i) \quad \sum_{i=1}^3 f_i = 1 \quad (\text{S2})$$

Examples of such fits are provided in Fig. S3. Both functions fit the data to within expected uncertainties of  $\pm 0.1$ - $0.2$  for  $t < 1$  ps and  $\pm 0.05$  at later times. The use of two fitting functions provides some measure of the uncertainties in the characteristic times derived from the fits.

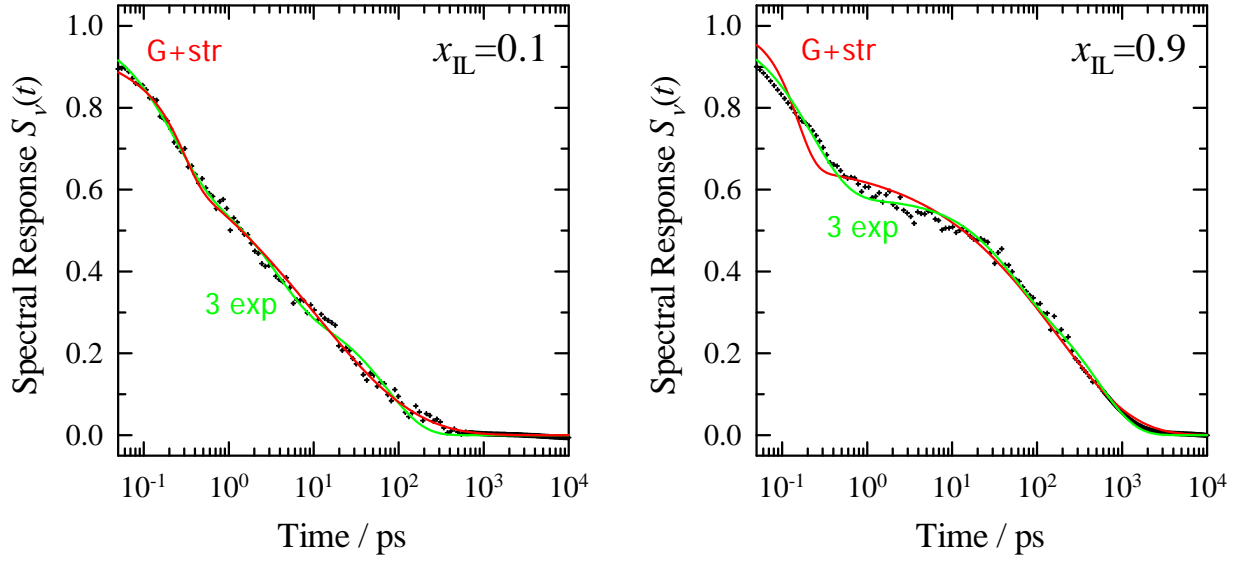


**Fig. S3:** Representative fits of  $S_v(t)$  data (points) to Eq. S1 (red curves, “G+str”) and Eq. S2 (green curves, “3 exp”).

Table S2 lists the parameters derived from both fits as well as three characteristic times determined from averages over the two functions. In the case of the Gaussian + stretched exponential function the fast time was determined from  $\tau_f = (\pi/2)^{1/2} \omega_G^{-1}$  and the (integral) slow time by  $\langle \tau_s \rangle = (\tau_0 / \beta) \Gamma(1/\beta)$ . In the case of the triple exponential function, these times were determined from  $\tau_f = \tau_1$  and  $\langle \tau_s \rangle = \sum_{i=2,3} f_i \tau_i / \sum_{i=2,3} f_i$ .

**Table S2: Parameters of Fits to  $S_{\nu}(t)$  Data (20.5 °C)**

<b>A. Fits to Eq. S1 - Gaussian + Stretched Exponential Function</b>							
$x_{IL}$	$f_G$	$\omega_G$	$\tau_0$	$\beta$	$\tau_f$	$\langle \tau_s \rangle$	$\langle \tau_{solv} \rangle$
0.05	0.16	50	0.4	0.22	0.03	23	19
0.1	0.19	4.7	10	0.37	0.27	44	36
0.3	0.09	8.5	12	0.31	0.15	89	81
0.5	0.25	9.7	30	0.36	0.13	141	106
0.7	0.35	16	76	0.41	0.08	231	151
0.9	0.33	9.3	170	0.48	0.14	362	243
1	0.32	6.1	183	0.47	0.20	421	287

<b>B. Fits to Eq. S2 - Triple Exponential Function</b>								
$x_{IL}$	$f_1$	$\tau_1$	$f_2$	$\tau_2$	$f_3$	$\tau_3$	$\langle \tau_s \rangle$	$\langle \tau_{solv} \rangle$
0.05	0.560	0.01	0.264	0.7	0.175	35	14	6
0.1	0.388	0.22	0.303	3.4	0.309	73	38	24
0.3	0.379	0.13	0.258	4.7	0.363	94	57	35
0.5	0.457	0.19	0.254	14	0.289	213	120	65
0.7	0.471	0.13	0.215	20	0.314	328	203	107
0.9	0.420	0.23	0.228	44	0.351	525	336	195
1	0.409	0.33	0.288	49	0.303	743	405	240

<b>C. Times Summary</b>						
$x_{IL}$	$\Phi_{IL}$	$\eta$ /mPa	$\sigma^1$ /Ω m	$\tau_f$	$\langle \tau_s \rangle$	$\langle \tau_{solv} \rangle$
0.05	0.35	1.9	0.201	0.02±.02	18±8	13±2
0.1	0.54	2.9	0.190	0.24±.10	41±6	30±4
0.3	0.82	7.4	0.288	0.14±.06	73±32	58±9
0.5	0.91	15.5	0.486	0.16±.06	131±21	86±13
0.7	0.96	32.6	0.888	0.10±.05	217±33	129±19
0.9	0.99	72.8	2.091	0.18±.09	349±52	219±33
1	1	110	4.448	0.27±.13	413±62	263±39

All times are in units of ps and  $\omega_G$  in units of ps<sup>-1</sup>.  $\eta$  and  $\sigma^1$  are parameterized values of the viscosity and resistivity (25 °C) used to produce Figs. 7-8.

**D) Approximating the High-Frequency Components of  $\epsilon(\nu)$ :** In order to compensate the lack of the dielectric data in the high-frequency ( $\nu > 89$  GHz) region, we have augmented the mixture data using available dielectric data on the pure component liquids. For this purpose the 200 MHz-3THz data of Stoppa *et al.*<sup>2</sup> for [Im<sub>41</sub>][BF<sub>4</sub>] and the compilation and analysis of water dielectric data to 25 THz by Ellison<sup>3</sup> were used. We extended the mixture dielectric data in the following manner:

$$\hat{\epsilon}(p) = \hat{\epsilon}^{MW}(p) - \epsilon_{\infty}^{MW} + (\epsilon_{\infty}^{MW} - n_D^2) \{ \Phi_{IL} \delta \hat{\epsilon}_{IL}(p) + (1 - \Phi_{IL}) \delta \hat{\epsilon}_W(p) \} + n_D^2 \quad (S3)$$

In these equations  $p = i2\pi\nu$ ,  $\hat{\epsilon}^{MW}(p)$  is the 4-Debye representation of the observed mixture data, and  $n_D$  is the refractive index of the mixture. We approximate the missing component of the dielectric response due to neat [Im<sub>41</sub>][BF<sub>4</sub>],  $\delta \hat{\epsilon}_{IL}$ , using a single resonance term,

$$\delta \hat{\epsilon}_{IL}(p) = \frac{\nu_0^2}{\nu_0^2 + p(p + \gamma)} \quad (S4)$$

with parameters  $\nu_0 = 2.85$  THz and  $\gamma = 4.85$  THz.<sup>2</sup> The missing component of water,  $\delta \hat{\epsilon}_W$ , includes those components of the neat water response occurring above 89 GHz, which was parameterized by Ellison to include one Debye relaxation term and two resonance terms:

$$\delta \hat{\epsilon}(p) = \frac{1}{\Delta_3 + \Delta_4 + \Delta_5} \left\{ \frac{\Delta_3}{1 - p\tau_3} + \frac{\Delta_4(1 + \varpi_4^2 - p\tau_4)}{\varpi_4^2 + (1 - p\tau_4)^2} + \frac{\Delta_5(1 + \varpi_5^2 - p\tau_5)}{\varpi_5^2 + (1 - p\tau_5)^2} \right\} \quad (S5)$$

with  $\varpi_i = 2\pi\tau_i f_i$  and parameters appropriate to 25 °C tabulated below.

	$i=3$	$i=4$	$i=5$
$\Delta_i$	1.3779	0.6769	0.7380
$\tau_i / 10^{-14}$ s	8.1853	9.7444	2.3174
$f_i / 10^{12}$ s <sup>-1</sup>	--	4.0310	14.434

Figure S4 shows an example of this high-frequency supplement for the case  $x_{IL} = 0.5$  and Fig. S5 shows the parameterized and estimated dielectric data of all of the mixtures used for comparison to solvation data.

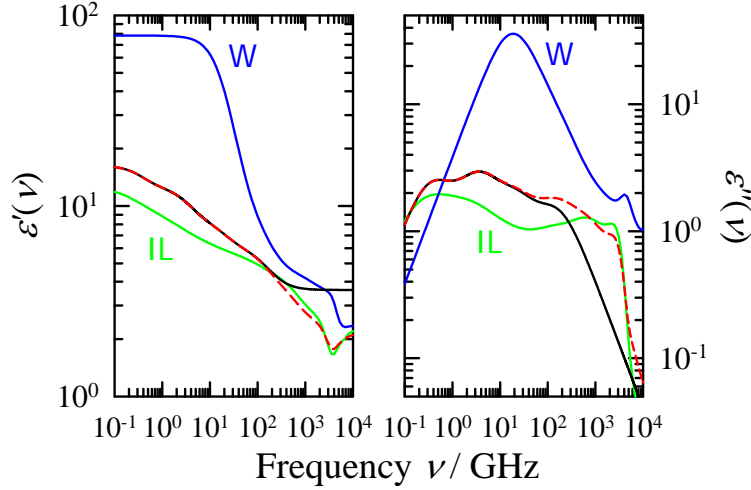


**Fig. S4:** Estimating the high-frequency portion of the dielectric permittivity and dielectric loss for the case  $x_{IL} = 0.5$ . Blue and green curves are  $\epsilon(\nu)$  in neat water and  $[\text{Im}_{41}][\text{BF}_4]$  respectively. The black curve is  $\epsilon^{MW}(\nu)$  measured to 89 GHz and represented by a 4-Debye function (Eq. 3-3) and the dashed red curve is  $\epsilon(\nu)$  estimated according to Eqs. S3-S5.

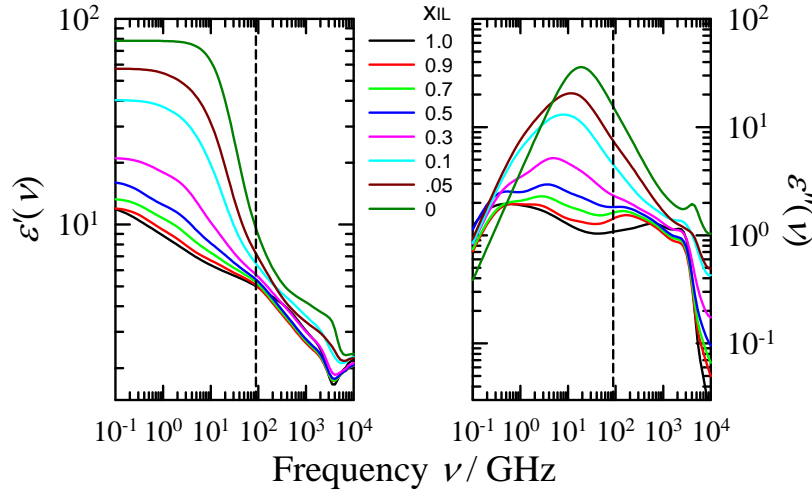


**Fig. S5:** Dielectric permittivity and loss for the entire mixture series after estimating the high-frequency data according to Eqs. S3-S5. The dashed lines indicate the 89 GHz limit of the measured mixture data.

Koeberg *et al.*<sup>4</sup> used terahertz time-domain ultrafast spectroscopy to measure the dielectric spectra of  $[\text{Im}_{41}][\text{BF}_4]$  over the frequency range 0.1-1.2 THz. Figure S6 shows some comparisons of their data to the high-frequency estimates employed here. The compositions at which these comparisons are made are not exact matches. The values of  $x_{IL}$  used are (this work, Koeberg): (.893, .905), (.492, .493), (.282, .319), (.105, .109), and (.050, .038). As shown in Fig. S6, the agreement between the two data sets is generally good. At 100 GHz, just slightly

above our high-frequency limit and also the low-frequency end of the Koeberg data, we find that values of  $\varepsilon'$  and  $\varepsilon''$  differ by an average of 5% and 23% respectively. The extrapolations above 100 GHz used here agree with the terahertz data to a similar extent but also include some small resonance contributions at frequencies higher than 1.2 THz that are not captured in the latter data.

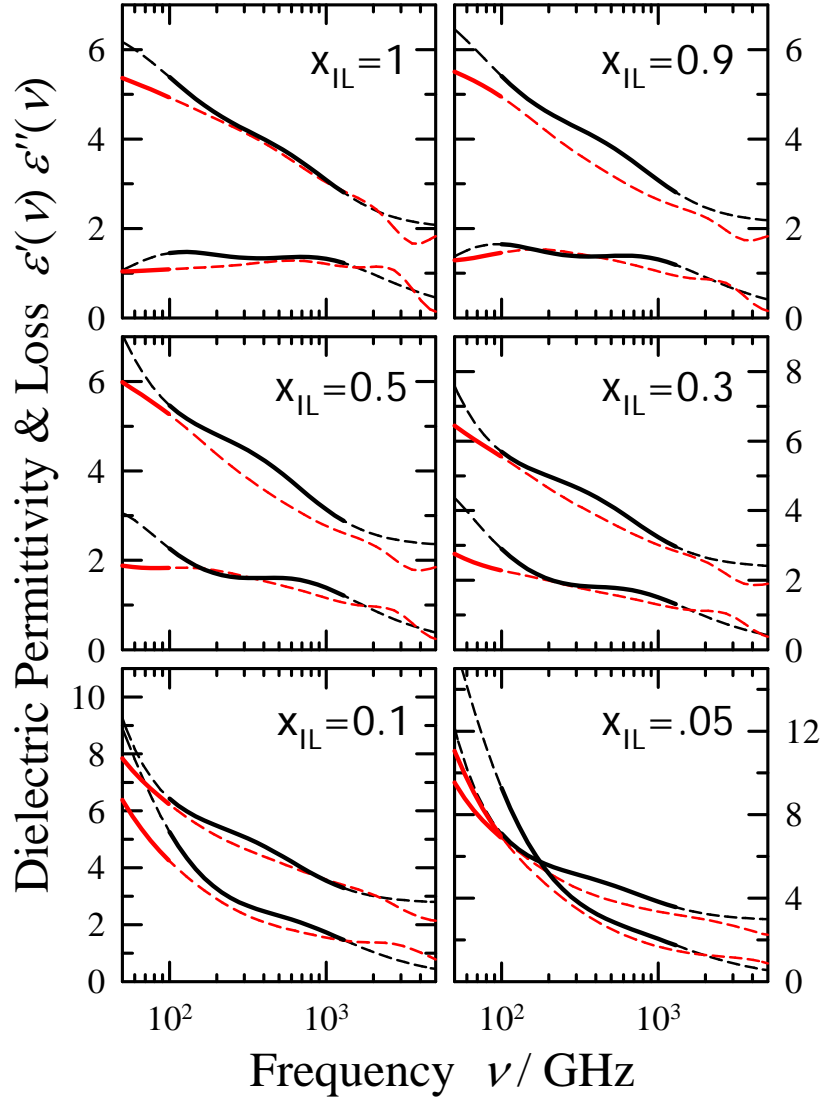


**Fig. S6:** Comparison of the dielectric data reported here and its extrapolation to THz frequencies (red curves) with the data of Koeberg *et al.*<sup>4</sup> (black curves). The heavy solid curves indicate the frequency range over which data were recorded and the lighter dashed curves the fitted functions used to represent and extrapolate the data. Upper curves at high  $\nu$  correspond to  $\varepsilon'(\nu)$  and lower curves to  $\varepsilon''(\nu)$ . The conductivity correction (Eq. 2) was not applied to the data reported by Koeberg *et al.* (private communication) but we have made this correction here for consistency with our representation.



**D) Comparisons of Dielectric Continuum Predictions for  $S(t)$  and Observed Data:**

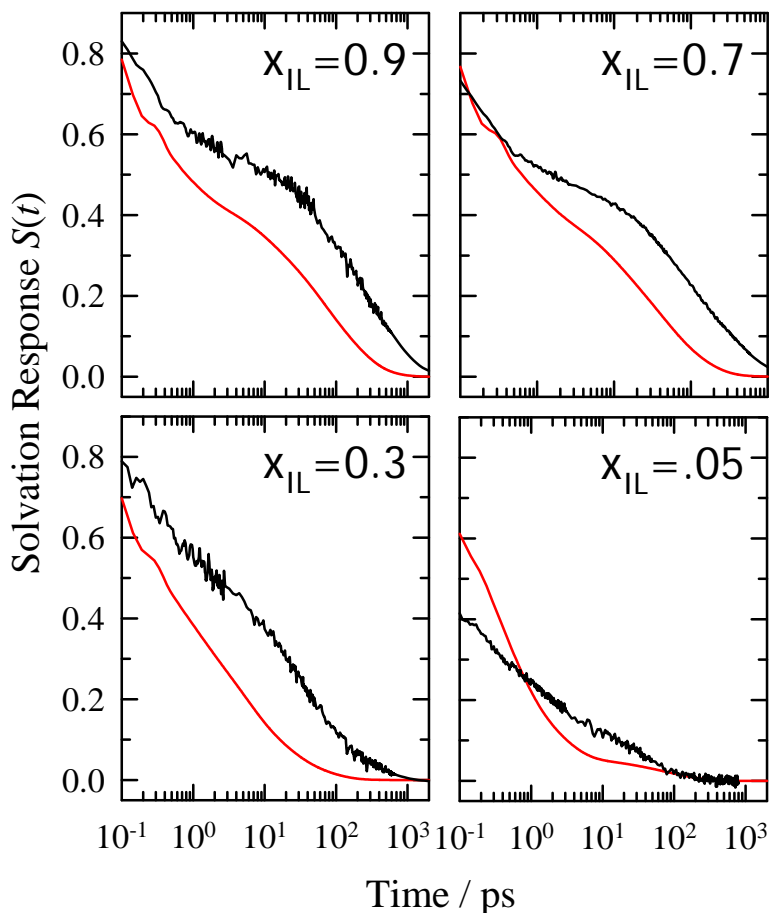


**Fig. S7:** Some direct comparisons of observed spectral response functions  $S_i(t)$  (black) and response functions calculated using the dielectric continuum model ( $S(t)$ , red).

**References:**

1. M. M. Taib and T. Murugesan, "Density, Refractive Index, and Excess Properties of 1-Butyl-3-methylimidazolium Tetrafluoroborate with Water and Monoethanolamine," *J. Chem. Eng. Data* **57**, 120-126 (2011).
2. A. Stoppa, J. Hunger, R. Buchner, G. Heftner, A. Thoman, and H. Helm, "Interactions and Dynamics in Ionic Liquids," *J. Phys. Chem. B* **112**, 4854-4858 (2008).
3. W. J. Ellison, "Permittivity of pure water, at standard atmospheric pressure, over the frequency range 0-25 THz and the temperature range 0-100°C," *J. Phys. Chem. Ref. Data* **36**, 1-18 (2007).
4. M. Koeberg, C.-C. Wu, D. Kim, and M. Bonn, "THz dielectric relaxation of ionic liquid:water mixtures," *Chem. Phys. Lett.* **439**, 60-64 (2007).